Ultrasound and photoacoustic analysis of cell pellets at 200 MHz

Lauren A. Wirtzfeld, Eric M. Strohm, Michael C. Kolios*

Department of Physics, Ryerson University, Toronto, Ontario, Canada
Institute for Biomedical Engineering, Science and Technology (iBEST), a partnership between Ryerson University and St. Michael's Hospital, Toronto, Canada
Keenan Research Centre for Biomedical Science of St. Michael's Hospital, Toronto, Canada
*mkolios@ryerson.ca

***Abstract*— The complex scattering of ultrasound from biological tissues is not fully understood. The relationship between tissue structure and scattering is further complicated by variations in scattering sources and number density with varied imaging frequency. Above 100 MHz, where the resolution volume is on the order of a cell, single cells have been well studied, but not collections of cells. Over the range of 20 MHz to 80 MHz, where the resolution volume contains a number of cells, in vitro models of packed cells have been studied and characterized. This study presents ultrasound and photoacoustic data from three-dimensionally packed cell pellets at 200 MHz, where the resolution volume is on the order of the size of the cell nucleus. Dyes were used to obtain photoacoustic signal from either the nucleus or cytoplasm of the cells. B-mode images with good signal to noise ratio were obtained from both photoacoustic and ultrasound images. Speckle patterns were seen on both photoacoustic and ultrasound images, suggesting that echoes from multiple scatterers or sources are received despite the small resolution volume, comparable to the size of a cell nucleus. Power spectra show many features over the transducer bandwidth, which will be a focus of future work to analyze the acoustic backscatter and photoacoustic signal spectra.**

Keywords—Photoacoustics; High-Frequency Ultrasound; HT-29; AML; Cell Pellets

I. Introduction

Ultrasonic scattering from tissue is not a fully understood phenomenon; the complexities of tissue structure and composition make it difficult to understand the contributions of individual components to overall backscatter. However, the ability to characterize these subtle differences across tissues could have a significant clinical impact by aiding diagnostics. Changes at the cellular level could have clinical significance, such as changes in the nucleus to cytoplasm ratio of cancer cells compared to normal cells. The ability to provide detailed cellular analysis using non-invasive imaging methods could provide diagnostic value. Ultrasound and photoacoustic imaging are complementary techniques that are capable of detecting cellular level changes [1]–[3].

Increasing the ultrasound frequency improves the image resolution, but this also changes the relationship between the beam and scatterer size. As the resolution approaches the size of the cell or nucleus, the ultrasound scattering behavior changes and assumptions based on backscatter from large collections of cells within the resolution volume of the transducer no longer hold. Ultrasound and photoacoustic imaging of single cells from 200 MHz to 1000 MHz has produced high resolution single cell images, giving detailed information on the acoustic and optical parameters with good agreement to theoretical calculations [3], [4]. Work on ultrasound characterization using *in-vitro* arrangements of cells in three-dimensional (3D) pellets and gels have been performed over a range up frequencies from 20-80 MHz [5]–[7]. Increasing the imaging frequency from 50 MHz, which has a few cells within a resolution volume, to 200 MHz, which has a resolution volume similar to that of a single nucleus, will change how ultrasound scatters from the collections of cells. Whereas ultrasound data will contain scattering from a variety of structures on the cellular to subcellular level, the source of the photoacoustic signals can be controlled by using localized dyes particular to specific cellular structures. In particular, photoacoustic signal can be selectively obtained from the nucleus or the cytoplasm allowing for a comparison of the photoacoustic signals with the ultrasound backscatter data from the same sample.

In this study, ultrasound and photoacoustic measurements of the same cell pellets were made at 200 MHz for the first

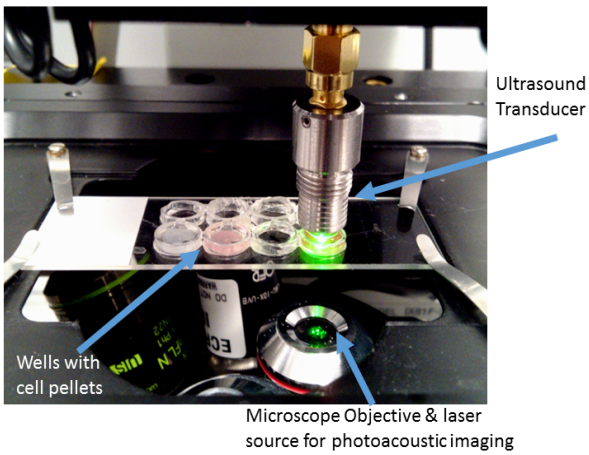

Fig. 1. Experimental setup for photoacoustic and ultrasound imaging of cell pellets. The sample is illuminated from the bottom for photoacoustics and the ultrasound transducer receives signals from the top of the sample. The same transducer is used in pulse echo mode.

978-1-4673-9897-8/16/$31.00 ©2016 IEEE

time. Two cell lines were used, in which the cell diameter and nuclear to cytoplasm ratio were different. The cells were dyed so that either the nucleus or cytoplasm generated the photoacoustic signals. B-mode images, RF signals and power spectra are presented for both ultrasound imaging and photoacoustic imaging (using a cellular and nuclear dye to create the photoacoustic signal) of the same cell pellets.

II. METHODS

HT-29 (human colon carcinoma) and OCI-AML5 (human acute myeloid leukemia) cells were dyed with DRAQ5, a nuclear dye; Neutral Red, a cytoplasmic dye; or left undyed. Both dyes were supravital and could penetrate the membrane of live cells. The two cell lines were chosen due to their different size and nucleus to cytoplasm ratio. The HT-29 have a larger outer diameter than the AML cells (18.6 µm versus 9.8 µm, measured by a Coulter Counter). Both cell lines have a similar sized nucleus (~ 8 µm).

A custom holder was built with 6.5 mm diameter wells and a glass slide bottom, to allow both ultrasound and photoacoustic imaging. Approximately 2 to 3 million cells, were transferred to a well and the holder was centrifuged at approximately 200 g for 10 minutes to form the cell pellets.

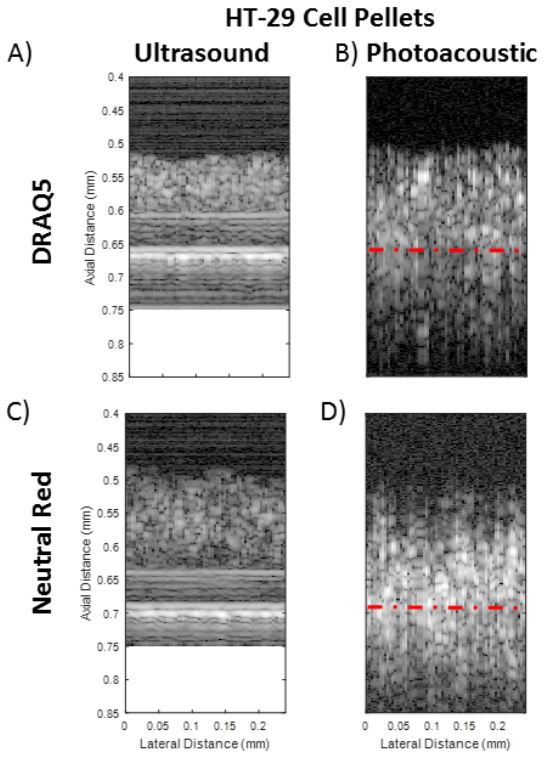

Fig. 2 Ultrasound (A & C) and Photoacoustic (B & D) B-mode images of a HT-29 cell pellet with the nuclei stained with DRAQ5 (A & B) or the cytoplasm stained with Neutral Red (C & D). A & B Show an artifact above the strong reflection from the glass bottom of the well. B & D Show a mirrored photoacoustic image. Scales are the same on all images. The red dashed line approximates the location of bottom of the well in the photoacoustic images.

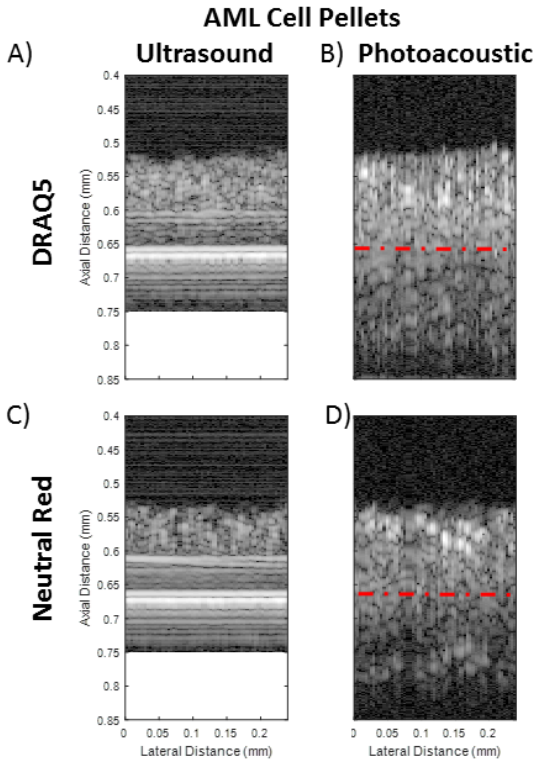

Fig. 2. Ultrasound (A & C) and Photoacoustic (B & D) B-mode images of an AML cell pellet with the nuclei stained with DRAQ5 (A & B) or the cytoplasm stained with Neutral Red (C & D). The red dashed line approximates the location of bottom of the well in the photoacoustic images.

Pellets were approximate 150 µm thick.

Pellets were imaged with a photoacoustic microscope (Fig.1) that was designed and built by Kibero GmbH (Saarbrucken, Germany), using a 200 MHz f#1 transducer and a 532 nm pulsed laser[3]. Both the ultrasound and laser were focused at the center of the pellets for the measurements, with the laser illuminating the sample from the bottom and the ultrasound measurements recorded from the top. This allowed for the imaging field of view to cover the entire cell, with ultrasound backscatter from the entire pellet to be obtained, as well as photoacoustic signals from either the nucleus or cytoplasm, which was dependent on where the dye would localize in the cells. Pellets of dyed cells were imaged in both ultrasound and photoacoustic mode, whereas undyed cells were only imaged in ultrasound mode. Each acquired scan line was the average of 100 acquisitions with the data bandpass filtered from 100 MHz to 800 MHz and time windowed around the signals received from the cell pellet for a total length of 500 ns. For each scan, RF data was acquired over a 248 µm by 248 µm region in 4 µm steps, with B-mode images reconstructed from the 62 scanlines collected along one plane.

III. RESULTS & DISCUSSION

Reconstructed B-mode ultrasound and photoacoustic images all show speckle throughout the cell pellet (Fig. 2-3)

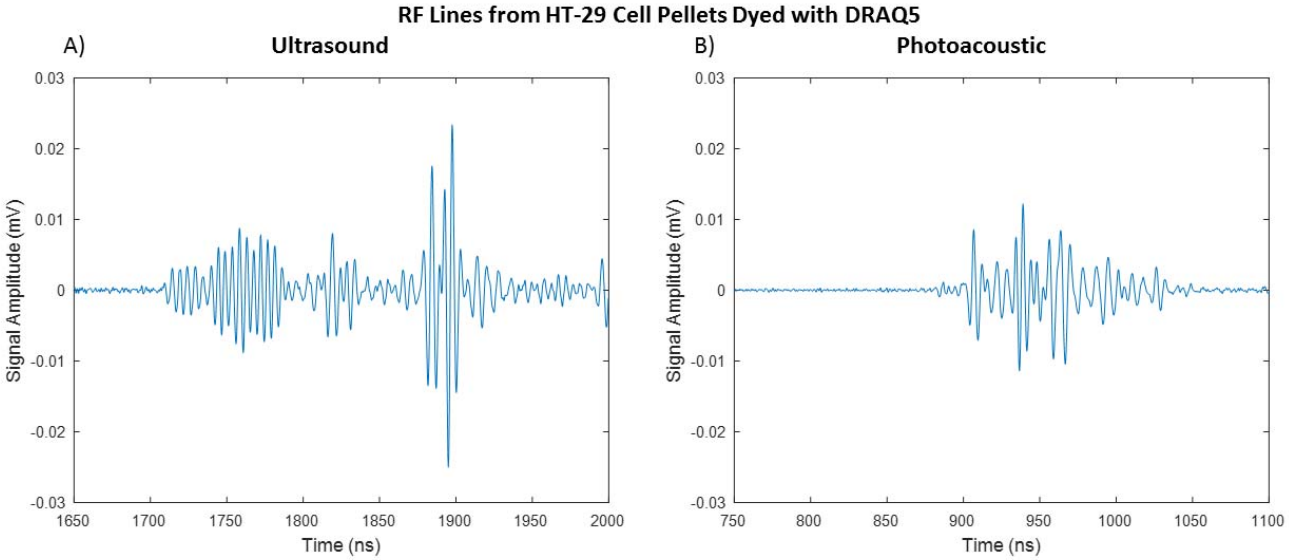

Fig. 4. Representative A) ultrasound and B) photoacoustic RF lines from a HT-29 cell pellet with the nuclei dyed with DRAQ5. Signals correspond to B-mode images shown in Figure 2. Note that the axes are the same for both the ultrasound and photoacoustic data.

with good signal to noise ratio. The ultrasound images (Fig. 2A/C, Fig. 3A/C) clearly show the glass slide at the bottom of the well at 0.65 mm, with an additional bright line above the glass slide arising due to the rim echo artifact common in these transducers. In the photoacoustic images (Fig. 2B/D, Fig. 3B/D), the glass slide is not visible and the pellets appear larger due to a mirroring effect, with the glass slide acting as the mirror. The mirroring effect is particularly noticeable in Figure 2B where the bright region at the top left of centre is seen also at the bottom of the pellet. The neutral red dye (Figure 4C/D, Figure 5C/D) absorbed the incident laser light more than the DRAQ5 dye, which resulted in greater light attenuation and a lower photoacoustic signal at the top surface of the pellet (since the light was incident from the bottom of the well).

Representative RF-lines from the DRAQ5 dyed HT-29 pellet are plotted in Figure 4 (individual data lines are from the B-mode image of Figure 2 A/B). The signal amplitude from the ultrasound and photoacoustic experiments was of comparable magnitude within the pellet, with the reflection from the bottom of well just after 0.65 mm in ultrasound. The mirror plane in the photoacoustics corresponds to the location of the bottom of the well and the approximate location is indicated with a red dashed line in the figures. The effect of the wider bandwidth signal in photoacoustics is notable in the RF, with the lower frequency components compared to the ultrasound RF (greater distance between peaks). The corresponding power spectra, with maxima normalized to 0 dB, are plotted in Figure 5 and show complex spectral patterns with several features throughout the transducer bandwidth. There is variability between the spectra from different RF scanlines. As each RF line is made up of signals from a small number of cells due to the small resolution volume, the number and configuration of cells interrogated for each RF line may vary significantly during the transducer raster scan over the sample, causing the variations observed in the power spectra. Despite these local variations and the small resolution volume, the clear speckle patterns in both the ultrasound and photoacoustic images indicate that signals from multiple scatterers or sources are being received. The scattering from several cells in the ultrasound depth of field as well as the potential off-axis cells illuminated in photoacoustics may contribute to the development of the speckle pattern obtained.

The work presented here demonstrates that high signal to noise can be obtained using 200 MHz from pellets of cells using both ultrasound and photoacoustics, where the ultrasound scattering and photoacoustic signal generation can be altered by using specific cell types or dyes. Analysis of these signals in future work will help us understand how the photoacoustic and ultrasound signals can be related, to better understand scattering phenomena in the application of fundamental theory to diagnostic ultrasound.

IV. CONCLUSIONS

Three dimensional arrangements of cells in tissue-mimicking pellets were imaged with ultrasound and photoacoustics at 200 MHz. Images with speckle patterns and good signal to noise were obtained from both photoacoustic and ultrasound data. Future work will focus on signal and spectral analysis techniques to evaluate structural and organizational parameters within the samples.

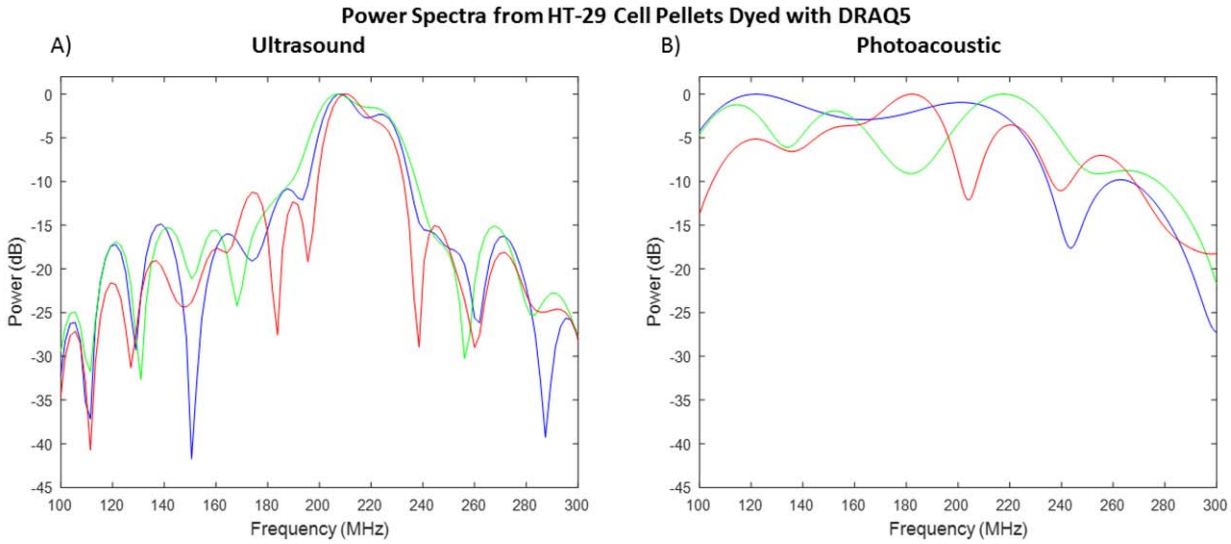

Fig. 5. Three representative ultrasound (A) and photoacoustic (B) power spectra from a HT-29 cell pellet with the nuclei dyed with DRAQ5. Both sets of data show features and distinct minima in the spectra with variability among scan-lines. Figures correspond to RF data in Figure 4 and B-mode images in Figure 2 A-B.

ACKNOWLEDGMENT

The authors would like to acknowledge funding from the Terry Fox Research Institute. Funding to purchase equipment was provided by the Canada Foundation for Innovation, the Ontario Ministry of Research and Innovation, and Ryerson University.

REFERENCES

[1] G. J. Czarnota, M. C. Kolios, H. Vaziri, S. Benchimol, F. P. Ottensmeyer, M. D. Sherar, and J. W. Hunt, "Ultrasonic biomicroscopy of viable, dead and apoptotic cells," *Ultrasound Med. Biol.*, vol. 23, no. 6, pp. 961–965, 1997.

[2] E. Strohm, G. J. Czarnota, and M. C. Kolios, "Quantitative measurements of apoptotic cell properties using acoustic microscopy," *IEEE Trans. Ultrason. Ferroelectr. Freq. Control*, vol. 57, no. 10, pp. 2293–2304, Oct. 2010.

[3] E. M. Strohm, M. J. Moore, and M. C. Kolios, "High resolution ultrasound and photoacoustic imaging of single cells," *Photoacoustics*, vol. 4, no. 1, pp. 36–42, Mar. 2016.

[4] M. Arakawa, J. Shikama, K. Yoshida, R. Nagaoka, K. Kobayashi, and Y. Saijo, "Development of an ultrasound microscope combined with optical microscope for multiparametric characterization of a single cell," *IEEE Trans. Ultrason. Ferroelectr. Freq. Control*, vol. 62, no. 9, pp. 1615–1622, Sep. 2015.

[5] A. Han, R. Abuhabsah, J. P. Blue, S. Sarwate, and W. D. O'Brien, "Ultrasonic backscatter coefficient quantitative estimates from high-concentration Chinese Hamster Ovary cell pellet biophantoms," *J. Acoust. Soc. Am.*, vol. 130, no. 6, pp. 4139–4147, Dec. 2011.

[6] M. C. Kolios, L. Taggart, R. E. Baddour, F. S. Foster, J. W. Hunt, G. J. Czarnota, and M. D. Sherar, "An investigation of backscatter power spectra from cells, cell pellets and microspheres," in *2003 IEEE Symposium on Ultrasonics*, 2003, vol. 1, p. 752–757 Vol.1.

[7] K. P. Mercado, M. Helguera, D. C. Hocking, and D. Dalecki, "Estimating Cell Concentration in Three-Dimensional Engineered Tissues Using High Frequency Quantitative Ultrasound," *Ann. Biomed. Eng.*, Mar. 2014.